JSES International 6 (2022) 447–453

Contents lists available at ScienceDirect

JSES International

journal homepage: www.jsesinternational.org

A lower critical coracoid process angle is associated with type-B osteoarthritis: a radiological study of normal and diseased shoulders

William Wynell-Mayow, MRCS[a,*], Chung Chi Chong [a], Omar Musbahi, MRCS[a,b], Edward Ibrahim, FRCS (Tr&Orth)[a]

[a]West Middlesex University Hospital, Chelsea and Westminster NHS Foundation Trust, Isleworth, Middlesex
[b]MSk Lab, White City Campus, Imperial College London, London

ARTICLE INFO

Keywords:
Shoulder anatomy
Critical shoulder angle
Critical coracoid process angle
Glenohumeral osteoarthritis
Scapular morphology
Glenoid wear
Rotator cuff tear

Level of evidence: Level III; Case-Control Cross-Sectional Design; Prognosis Study

Background: Degenerative rotator cuff tears and osteoarthritis (OA) are associated with differences in coronal plane scapular morphology, with particular focus on the effect of the critical shoulder angle (CSA) on shoulder biomechanics. The effect, if any, of axial plane scapular morphology is less well established. We have noticed wide disparity of axial coracoid tip position in relation to the face of the glenoid and sought to investigate the significance of this through measurement of the critical coracoid process angle (CCPA), which incorporates coracoid tip position and glenoid version.

Methods: CCPA, CSA, and glenoid retroversion were measured by three independent reviewers from the cross-sectional two-dimensional computed tomography (CT) and magnetic resonance imaging of 160 patients in four equal and matched case-control groups: (1) a control group of patients with a radiologically normal shoulder and no history of shoulder symptoms who had a CT thorax for another reason, (2) patients with primary OA with Walch type-A glenoid wear pattern on CT scan, (3) patients with type-B glenoid primary OA, and (4) patients with magnetic resonance imaging–proven atraumatic tears of the posterosuperior rotator cuff.

Results: Interobserver agreement was excellent for all measured parameters. The median CCPA was significantly lower in the type-B OA group (9.3°) than that in controls (18.7°), but not significantly different in the other study groups. There was a trend toward greater glenoid retroversion in the type-B OA group, but receiver operating characteristic curve analysis demonstrated the CCPA to be by far the most powerful discriminator for type-B OA. The optimal cutoff value was calculated for the CCPA at 14.3° with a sensitivity of 93% and specificity of 90% for type-B OA. Compared with controls, the CSA was significantly higher in the rotator cuff tear group and lower in both OA groups, but did not differentiate between type-A and type-B OA.

Conclusion: Combined with a lower CSA, a lower CCPA (<14.3°) is strongly predictive of type-B glenoid OA. The authors propose a simple model of pectoralis major biomechanics to explain the effect of this axial plane anatomical variation, which requires further investigation.

Degenerative rotator cuff tears (RCTs) and primary glenohumeral osteoarthritis (OA) are the two major age-related conditions affecting the shoulder.[33,34] There is a growing body of evidence to suggest that variations in individual scapular morphology significantly affect joint mechanics and likely play a significant role in the underlying disease processes.[5,19,32-34,40,43,52,53] Most focus has been on coronal plane variations that are associated with disease. This has been well described by the critical shoulder angle (CSA), which combines the acromion index and glenoid inclination into a single measurement.[34] A higher CSA (>35°) has been strongly associated with RCTs.[10,18,19,34,39,47,53,57] Conversely, a lower CSA (<30°) is found in patients with OA.[8,19,33,39,47,52]

The pattern of glenoid wear in primary glenohumeral OA shows greatest variation in the axial plane.[55] Walch has observed that the majority are either concentric (Walch type-A) or posterior eccentric (Walch type-B). Each type is subdivided as per the severity of glenoid erosion (A1-2; B1-3).[32,55] The hallmark of type-B OA is posterior humeral head subluxation, which has been proposed to begin as a dynamic phenomenon, progressing to static subluxation resulting in eccentric wear over time, suggesting a strong biomechanical influence.[14,54] This eccentric wear results in formation of a biconcave

Institutional review board approval was received from the HRA and Health and Care Research Wales (HCRW) Ethics committee (IRAS ID 288623).

*Corresponding author: William Wynell-Mayow, MRCS, Flat 317, West Block, Forum Magnum Square, London, SE1 7GL.
E-mail address: william.wynell-mayow@nhs.net (W. Wynell-Mayow).

https://doi.org/10.1016/j.jseint.2021.10.007

neo-glenoid and an acquired pathological glenoid retroversion (RV).[11,30,36,40,44] Other axial plane variations of scapular morphology associated with type-B OA have not yet been reported although abnormal coracoid morphology has been associated with glenoid dysplasia in obstetric brachial plexus palsy (OBPP).[26,35,38,46,51,58]

Through routine assessment of computed tomography (CT) scans in type-B OA, the senior author observed that the tip of the coracoid process is more medially placed in the axial plane with respect to the face of the glenoid. Individual variation in size and shape of the coracoid process has been well documented, particularly the association of increased lateral offset with RCTs, especially anterior tears.[17,28,41,49,59] An angle incorporating glenoid version and lateral coracoid offset (the 'critical coracoid process angle'; CCPA), akin to the CSA in the coronal plane, has been coined by Sada et al.[43] It is measured on axial cross-sectional imaging (CT or magnetic resonance imaging [MRI]) and reported to be associated with RCTs but has not been published in peer-reviewed literature or studied in the context of OA.

The aim of this study was to assess the association of the CCPA with type-A OA, type-B OA, and degenerative RCTs, as compared with the normal population.

Materials and methods

Study design and setting

This was a retrospective case-control study looking at patients who presented to a single trust in the United Kingdom between 2006 and 2020. Ethical approval was granted by the Health Research Authority (HRA IRAS ID: 288623).

Participants

All cross-sectional shoulder imaging of patients aged 60 years and above stored on our institution's picture archiving communication system (Marosis m-view, Marotech, Seoul, Korea) software from 2006 to 2020 was screened for the presence of either OA (CT scan) or RCT (MRI scan), as per the radiologist's report. Clinical notes were consulted to apply the following exclusion criteria: history of trauma, inflammatory joint disease, previous shoulder surgery, and duplicate scan of the same patient's shoulder. All CT scans reported as showing glenohumeral OA were categorized by the senior author as per the modified Walch classification.[6,55] Equal-sized case-control groups of matched imaging studies were then created (type-A OA, type-B OA, and RCTs). Type B3 (severe erosion) was excluded as there was no available glenoid landmark to accurately measure the CCPA. Type C (glenoid dysplasia) and type D (anterior wear) were excluded because of insufficiently observed numbers in our sample.

A matched group of controls was created from patients who had undergone a CT scan of the chest that happened to include the entire shoulder girdle, for reasons other than shoulder symptoms. Scans were chosen in order of the date performed, working from most recent backward. The clinical exclusion criteria were any documented history of shoulder disease, surgery, or trauma. The radiographic exclusion criteria were any prior shoulder imaging at our institution or any sign of degenerative or prior traumatic condition of the glenohumeral or subacromial articulations (eg, spur, cyst, osteophyte, sclerosis, narrowing, or fracture malunion).

Variables and data sources

Data extracted from scans included outcome characteristics based on radiologist reports and glenoid morphology (type-A OA, type-B OA, RCT, and control), confounding data for matching (age/sex/side) and radiological measurements performed on case-control groups.

Radiological measurements

CT and MRI images were viewed on a high-resolution liquid-crystal display LCD monitor using picture archiving communication system (Marosis m-view, Marotech, Seoul, Korea) software functionality to remove patient details, prior markings, and radiologist reports. MRI images were obtained from a Philips Achieva 1.5T scanner, and CT imaging procedures were performed on a Siemens Somatom Definition Edge using a single-energy CT protocol with a reconstructed slice thickness of 0.5 mm. All measurements performed on MRI were T1 or proton density–weighted images. All scans underwent predetermined multiplanar (axial, sagittal, and coronal) reformatting in the plane of the scapula body as per established methods.[16,23,42] (Fig. 1*A*).

As per previously described methods, three independent reviewers measured the CCPA[43] (Fig. 1*B*), CSA (Fig. 1*C*), and glenoid RV.[16,23,29,34] For the B2 subgroup, the paleo-glenoid, rather than neo-glenoid, was used to reference the face of the glenoid and, therefore, estimate the position of the paleo-glenoid posterior rim. The absence of the paleo-glenoid face in B3 glenoids rendered this measurement technique impossible and necessitated their exclusion in this study. Glenoids with insufficient paleo-glenoid to reference the glenoid face were considered B3 and excluded. Glenoid RV was also measured with reference to the paleo-glenoid face as described rather than the neo-glenoid because of the pathological bone loss in the B2 glenoid.[11,30,36,40,44] After interobserver reliability testing, a mean of the reviewer's results was used for investigation unless a significant difference (>20%) was identified in which case a repeat measurement was agreed by all three reviewers.

Bias

Bias was reduced by blinding of reviewers to assignment of the Walch glenoid type before measurements and to each other's measurements. Patient age, sex, side, and severity matching was also performed for each of the four case-control groups.

Study size

The study included 160 patients in matched case-control groups of 40 (type-A OA, type-B OA, RCT, and control). This sample size was reached based on similar studies conducted.[34,43,47,49] Group characteristics were defined by the scans displaying type-B2 OA, rarest of the studied pathologies. Twenty B2 glenoids were added to 20 B1 glenoids chosen by order of the scan date, to create a group of 40 type-B glenoids. A group of 40 type-A glenoids was then created matched to the type-B group for patient age, sex, side, and severity of erosion (A1 vs. A2). The same process was followed to create the RCT group. As per the classification system proposed by Cofield, large and massive tears were considered severe.[12]

Statistical methods

Results were recorded through Microsoft Excel, and statistical analysis was performed with the SPSS statistical software (IBM, Armonk, NY, USA) and STATA (version 11; Stata Corp, College Station, TX, USA). Normality testing was assessed using visual comparison of plotted data and Shapiro-Wilk test of normality. All angle analyses were treated as nonparametric. Median difference and 95% confidence intervals (CI) were calculated via the Hodges-Lehmann estimator and compared using Mann-Whitney U

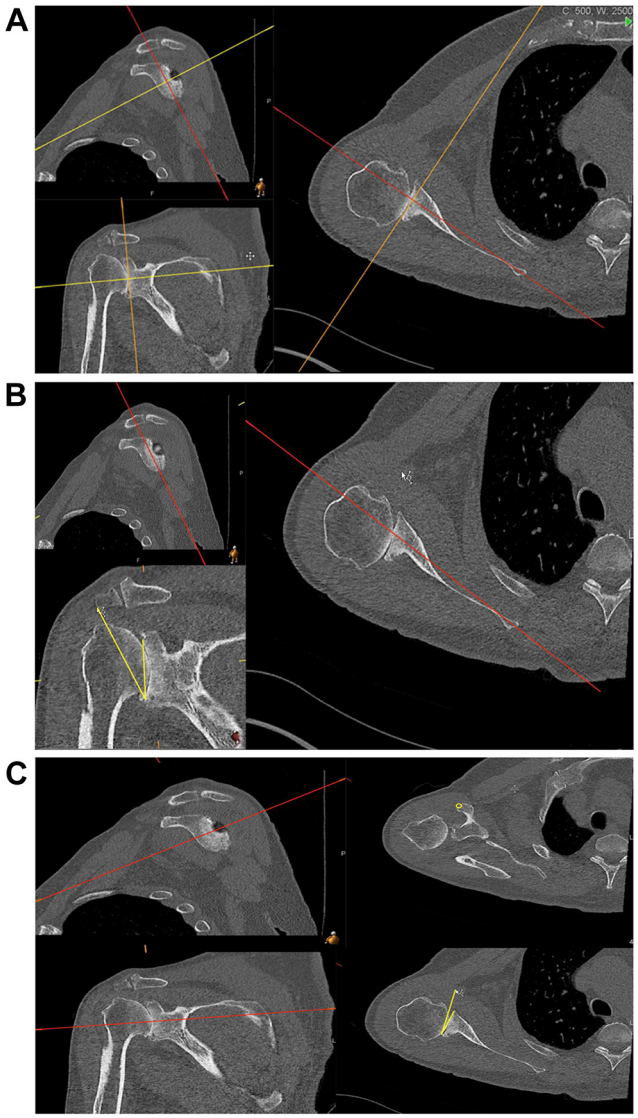

Figure 1 (**a**) Multiplanar reformatting of shoulder CT scans as per the plane of the scapula body. (**b**) The CSA measured in the coronal plane on multiplanar reformatted CT scans. The angle is formed from the most superior point of the glenoid rim to the most inferior point of the glenoid rim, to most infero-lateral projection of the acromion (yellow lines). (**c**) The CCPA measured in the axial plane on multiplanar reformatted CT scans. The angle is formed from the most anterior point of the glenoid rim to the most posterior point of the glenoid rim, at the level of the mid glenoid, to most antero-medial projection of the coracoid (yellow circle and lines). *CT*, computed tomography; *CCPA*, critical coracoid process angle; *CSA*, critical shoulder angle.

tests at a significant level of 0.05. Demographic data were normality distributed and were analyzed using Student's T test and chi-squared test where appropriate. Receiver operating characteristic (ROC) curve analysis was performed to find cutoffs and compare CCPA, CSA, and glenoid RV as discriminators between type-B OA and controls.

Interobserver reliability of the measurements was assessed by calculating the intraclass correlation coefficient (ICC) of each parameter using the two-way mixed-effects model. We considered ICCs of 0.7 or higher to be sufficient for the reliability as in similar studies.[9]

Results

The groups were well matched for baseline characteristics (Table I). Interobserver agreement between the three reviewers was demonstrated to be excellent for both CCPA and CSA measurements (ICC_{CCPA}, 0.980; ICC_{CSA}, 0.960). Table II highlights the average and observed distribution of CCPA, CSA, and RV for the four patient groups (Table II).

The CCPA was significantly lower in patients with type-B OA than that in controls (9.3° vs. 18.7°, respectively, $P < .05$) (Tables II and III). Shoulders with greater severity of posterior erosion had a lower median CCPA, but this did not reach statistical significance (B1; 10.1 [7.9-12.0] vs. B2; 7.6 [5.2-10.0], $P = .27$). There was no significant difference of the CCPA between controls and patients with type-A OA ($P = .425$) or RCT ($P = .194$).

The median CSA was significantly higher in the RCT group and significantly lower for both OA groups than that in controls (Table II) (Table III). There was no significant difference between values for type-A and type-B OA groups (27.4° vs. 27.8°, respectively, $P = .736$). Subgroup analysis found no significant difference for the CSA between OA grade severity for either type-A (A1; 27.5 [26.3-29.2], A2; 27.1 [23.3-29.9], $P = .875$) or type-B groups (B1; 28.4 [25.8-30.8], B2; 26.8 [25.6-29.5] $P = .599$). Fig. 2 is a graphical depiction of the interplay between the CCPA and CSA for each group, presenting all the data along with the median and interquartile range. Patients with type-B OA have a lower CCPA and CSA, whereas those with RCT or type-A OA are discriminated from controls by the CSA alone.

Compared with controls, median glenoid RV was not significantly different in any of the study groups, but there was a trend toward increased RV in the type-B OA group (controls; 4.4°, type-A OA; 5.35 [$P = .315$], type-B OA; 5.5 [$P = .102$], RCT; 3.5 [$P = .780$]) (Tables II and III).

ROC curve analysis demonstrated the CCPA to be the best discriminator for type-B OA of all the measured values with the highest area under the curve (CCPA; 0.964 [95% CI 0.93-0.997], CSA; 0.734 [95% CI 0.623-0.85], glenoid RV 0.607 [95% CI 0.481-0.732]) (Fig. 3). The optimal cutoff value was calculated for the CCPA at 14.3° with a sensitivity of 93% and specificity of 90% for type-B OA when combined with a low CSA.

Discussion

This study has demonstrated that both the CCPA and CSA are very significantly smaller in patients with type-B OA, regardless of severity, than those in controls. This differs from type-A OA, where only the CSA is smaller. Although there was trend toward higher native glenoid RV measured from the paleo-glenoid face, this did not reach statistical significance, and ROC curve analysis demonstrated the CCPA to be a much more powerful independent discriminator of type-B OA. Patients with RCTs did not have a significantly higher CCPA. A possible explanation for this is a likely lower number of subscapularis (SSC) tears than in previous coracoid studies.[4,59] We purposefully did not classify cuff tears by the anatomical position as arthroscopy is the gold standard for this, and the accuracy of MRI for the detection of SSC tears is relatively low.[13,50]

The role of individual scapular morphology in the development of degenerative shoulder conditions has been an area of intense research over the last few years. Increasing evidence has indicated that underlying coronal plane variation is implicated in the progression of shoulder degeneration to either OA or RCTs, with previous findings with respect to the CSA replicated in this study.[8,10,18,19,33,34,39,47,53,57] This article sought to further understanding of axial plane scapular morphology and association with posterior wear patterns of OA. Glenoid RV has been suggested to be associated with posterior subluxation of the humeral head and type-B glenoid pattern of degenerative wear.[32,55] Multiple studies have suggested the glenoid RV to be an acquired rather than

Table I
Baseline characteristics of each group.

Demographic	Control	RCT	Type-A OA	Type-B OA
Number	40 [-]	40 [$P = 1.0$]	40 [$P = 1.0$]	40 [$P = 1.0$]
Severity low	-	20 [$P = 1.0$]	20 [$P = 1.0$]	20 [$P = 1.0$]
Severity high	-	20 [$P = 1.0$]	20 [$P = 1.0$]	20 [$P = 1.0$]
Age	72.1 (70.0 to 74.2) [-]	71.8 (70.2 to 73.3) [$P = .785$]	72.4 (70.4 to 74.4) [$P = .836$]	71.7 (69.2 to 74.1) [$P = .791$]
Female	27 [-]	26 [$P = .813$]	27 [$P = 1.0$]	26 [$P = .813$]
Male	13 [-]	14 [$P = .813$]	13 [$P = 1.0$]	14 [$P = .813$]
Left	22 [-]	22 [$P = 1.0$]	23 [$P = .823$]	21 [$P = .823$]
Right	18 [-]	18 [$P = 1.0$]	17 [$P = .823$]	19 [$P = .823$]

RCT, rotator cuff tear; *OA*, osteoarthritis.
Severity low (small/moderate cuff tear, A1 OA or B1 OA), severity high (large/massive cuff tear, A2 OA or B2 OA).
Age is presented as mean (CI). All other results presented as number (n). [*P* value by compared with the control group].

Table II
Median CCPA, CSA, and glenoid retroversion (degrees) across four patient groups.

Measurement	Control (n = 40)	RCT (n = 40)	Type-A OA (n = 40)	Type-B OA (n = 40)
CCPA	18.7 (16.4 to 20.5), SD 3.6	20.3 (16.8 to 22.6), SD 6.9	17.0 (12.5 to 23.5), SD 7.1	9.3 (6.3 to 11.3), SD 5.7
CSA	30.8 (28.9 to 32.0), SD 2.6	37 (34.1 to 38.4), SD 4.6	27.4 (24.2 to 29.7), SD 3.7	27.8 (25.5 to 30.6), SD 4.2
RV	4.4 (2.25 to 6.9), SD 3.4	3.5 (1.9 to 7.5), SD 3.4	5.35 (1.1 to 9.1), SD 5.9	5.5 (3.0 to 8.05), SD 3.8

RCT, rotator cuff tear group; *OA*, osteoarthritis; *CSA*, critical shoulder angle; *CCPA*, critical coracoid process angle; *RV*, retroversion; *SD*, standard deviation.
Median values (25% to 75% interquartile range).

Table III
Median difference of CCPA, CSA, and glenoid RV (degrees) between pathological shoulders and controls.

Measurement	RCT (n = 40)	Type-A OA (n = 40)	Type-B OA (n = 40)
CCPA	1.3 (95% CI -0.7 to 3.1) [$P = .194$]	-0.8 (95% CI -3.3 to 1.6) [$P = .425$]	-9.75 (95% CI -11.6 to -8.0) [$P < .05$]
CSA	6.2 (95% CI 4.8 to 7.6) [$P < .05$]	-3.3 (95% CI -4.7 to -1.87) [$P < .05$]	-2.67 (95% CI -4.2 to -1.2) [P < . 05]
RV	-3.0 (95% CI -1.8 to 1) [$P = .780$]	1.1 (95% CI -1.1 to 3.4) [$P = .315$]	1.3 (95% CI -0.3 to 2.9) [$P = .102$]

RCT, rotator cuff tear group; *OA*, osteoarthritis; *CSA*, critical shoulder angle; *CCPA*, critical coracoid process angle; *RV*, retroversion, *CI*, confidence interval.
Median difference (95% confidence intervals using the Hodges-Lehmann estimator) [*P* values vs. control using Mann-Whitney U test].

causal pathology due to posterior bone loss after static subluxation.[11,30,36,40,44]

The authors noticed patients with type-B OA tend to have a more medially positioned coracoid process tip. A combination of glenoid version and coracoid projection is taken into account with the CCPA.[44] This angle is defined as the angle subtended by three points: the anterior glenoid rim, the posterior glenoid rim, and the tip of the coracoid (Fig. 1*B*).[43] An equivalent angle called the coracoglenoid angle has been described by Asal et al and investigated with respect to SSC tendon pathology.[4] This references the anterior, rather than posterior, glenoid rim at the point of the angle. We prefer the CCPA as it is more akin to the CSA, which is well-known and easily remembered.

Glenohumeral stability is accepted to be provided by a combination of active and static restraints.[7] A muscle's ability to impart compression or sheer at a joint is a function of its line of action.[2,60] Biomechanical modeling of the CSA suggests that the position of the acromion dictates the deltoid (DLT) attachment and, therefore, its vector of pull.[52,53] Combined with variations in native glenoid inclination, this results in either repetitive excessive glenohumeral superior translation and subacromial impingement (resulting in RCT) or higher joint compression forces (resulting in OA).[21,33,34,48,52,53] Given the observed progression of type-B OA patterns from dynamic humeral head subluxation to static subluxation with eccentric glenoid wear, the authors suggest a similar model implicating the position of the coracoid tip combined with the glenoid version in the axial plane.[14,55,56] This study measured the glenoid version from the face of the paleo-glenoid allowed by the exclusion of the B3 glenoids with the insufficient paleo-glenoid to accurately measure the face. The exclusion of B3 glenoids and the use of the paleo- rather than pathologically acquired neo-glenoid are proposed to explain this study's lower level of association between glenoid RV and type-B OA than in the literature.[11,30,36,40,44]

Biomechanical studies have established pectoralis major (PM) as the major dynamic destabilizing force acting on the glenohumeral joint in the axial plane;[1-3,24,27,31,37] an electromyography study has shown increased activation of PM in patients with anterior instability.[21] Furthermore, section of the PM tendon and, more recently, botulinum toxin injection into the PM muscle bellies are established treatments for chronic recurrent anterior instability where other forms of surgery are not indicated.[15,22,45] A number of muscles (DLT, SSC, teres major) can produce dynamic posterior translation of which the middle DLT is the most significant potential posterior destabilizer, but it appears that no one single muscle is responsible for counterbalance of the PM.[2,22,27] It follows, therefore, that significant alterations in the vector of pull of the PM might result in imbalance between anterior and posterior translatory forces acting across the joint. As the PM converges on its tendinous insertion on the lateral lip of the bicipital groove of the humerus, it courses over the conjoint tendon of the short head of biceps and coracobrachialis, close to its coracoid insertion, in an arrangement reminiscent of a simple pulley mechanism (Fig. 4). The functional implication of this vector of the PM has been used as a biomechanical justification for PM transfer under, rather than over, the conjoint tendon in SSC-deficient shoulders.[25] We postulate that medial positioning of the coracoid tip reduces the pulley effect produced by the conjoint tendon, resulting in a smaller anterior force vector of the PM. Combined with normal or excessive glenoid

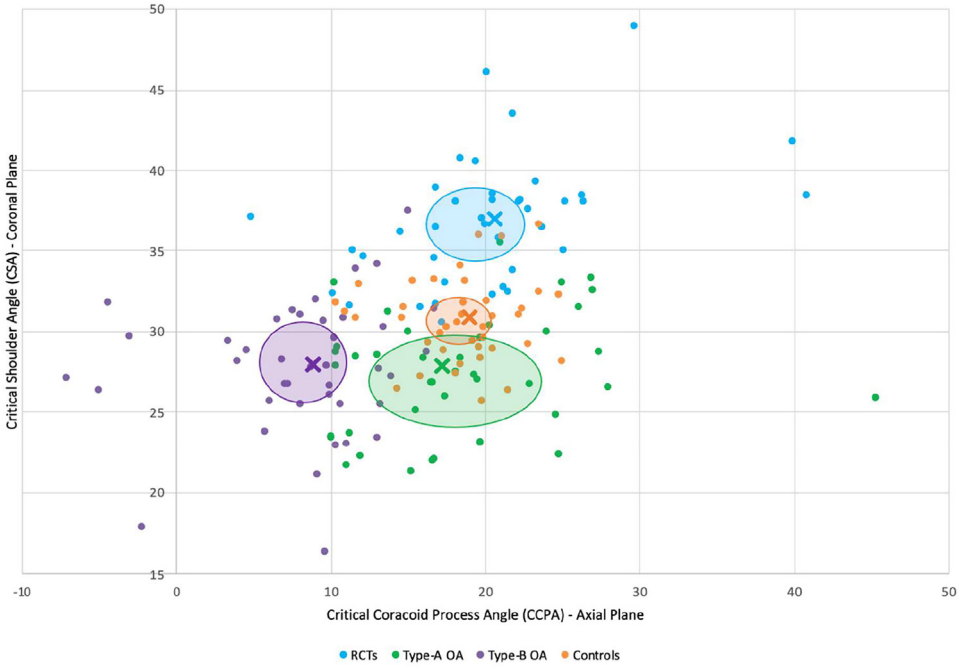

Figure 2 The scatter plot of the CSA against the CCPA to demonstrate the relationship of the two angles for each group. Each point represents a single scan—RCTs (blue), type-A OA (green), type-B OA (purple), and controls (orange); group median (**X**) and 25%-75% interquartile range (bubble). *RCT*, rotator cuff tear; *OA*, osteoarthritis.

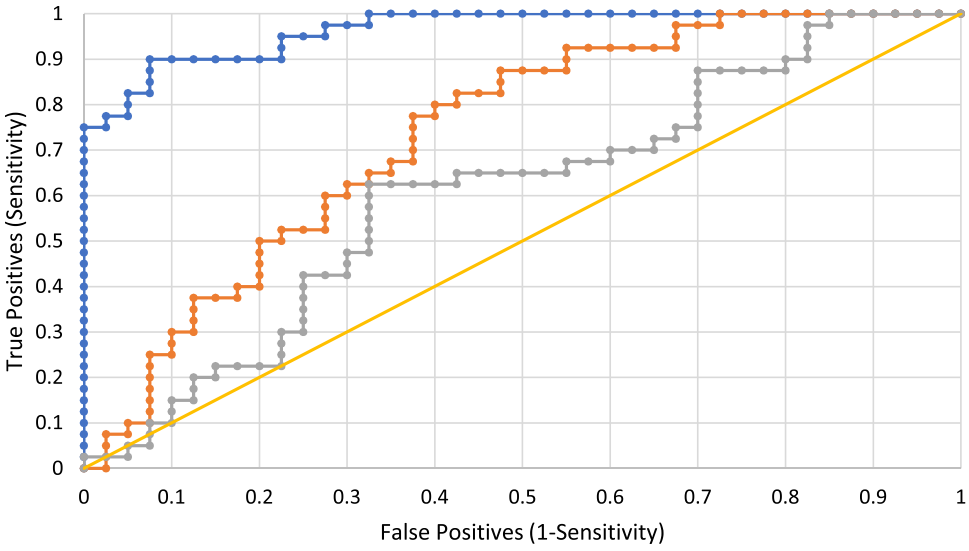

Figure 3 Receiver operating characteristic (ROC) curves for the critical coracoid process angle (CCPA) in blue, the critical shoulder angle (CSA) in orange, and the glenoid retroversion (RV) in gray for the prediction of type-B osteoarthritis. The reference line is indicated in yellow.

RV, this results in recurrent posterior translation of the humeral head (Fig. 4). When combined with the increased joint reaction force resultant from a low CSA, we suggest that a low CCPA contributes to the development of posterior OA wear patterns. Conversely, a normal CCPA with a more usual projecting coracoid is proposed to be protective in centralizing the humeral head and was associated either with type-A OA or with a normal shoulder in this study, depending on the value of the CSA.

Indirect support for our model comes from the observation of scapula dysplasia found in the shoulders of patients affected by OBPP. Significant increase in the coracoid overlap or lateral projection has been demonstrated in patients with OBPP who have a dysplastic retroverted glenoid and posterior subluxating humeral head.[26,35,38,46,51,58] Our model is suggestive that this lateral coracoid elongation might develop as a protective mechanism to maximize the anterior PM force vector. However, further biomechanical modeling and longitudinal cohort studies are needed to investigate the author's proposed theoretical model of the effect of the CCPA on glenohumeral forces. Further modeling of the sagittal plane scapular morphology may be beneficial in creating a 3-dimensional understanding of glenohumeral stability.

Limitations

This study is retrospective and, therefore, vulnerable to selection bias. This has been mitigated through the case-control study

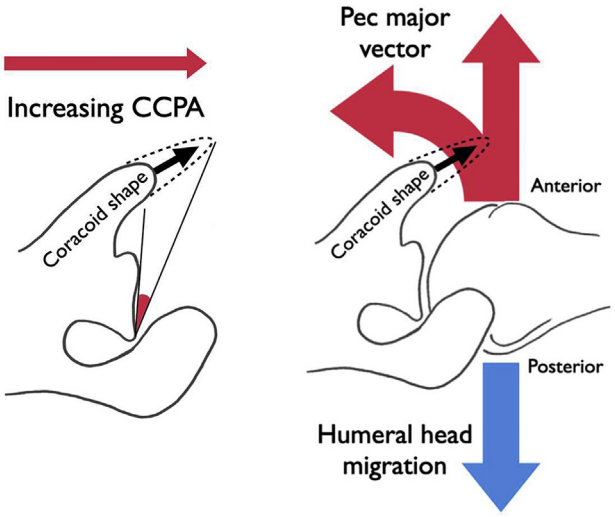

Figure 4 A medial position of the coracoid tip reduces the CCPA. This reduces the pulley effect on the pectoralis major as it slings over the conjoint tendon, resulting in reduced anterior translation force. The resulting imbalance results in excess posterior translation of the humeral head, which may be combined with excessive glenoid retroversion in some cases. *CCPA*, critical coracoid process angle.

design. The radiological inclusion/exclusion criteria for control scans were strict, although patients were not directly contacted about shoulder symptoms. The consistency of the CSA result with the literature indicates that the sample is representative of a typical patient population. When reviewing scans, the diagnosis of OA vs. RCT was usually obvious; however, blinding to assignment of type-A or type-B was possible for borderline cases. Scans compared were mixed modalities (CT/MRI); however, all patients with OA and control patients had a CT scan. Both CT and MRI have been validated as reliable comparable measures of scapula morphology with good interobserver and intraobserver reliability.[20] The most severe type-B3 glenoids or completely destructed unclassifiable glenoids were excluded because of a lack of landmarks for measurement and may be a source of bias. Type C and D glenoids were excluded because of low numbers; the relationship of the CCPA to these patterns is therefore unknown and an avenue for further research. A larger study including sufficient numbers of these less common and more dysplastic glenoid patterns may add further weight to the theory of altered PM biomechanics.

Conclusions

This study has evaluated and has demonstrated the association of a low CCPA, combined with a low CSA, in patients with type-B primary OA of the glenohumeral joint, whereas a normal CCPA and low CSA are associated with type-A OA. An abnormal CCPA was not associated with degenerative RCTs. The CCPA is a reliable radiological index, measured on cross-sectional imaging in the axial plane, incorporating coracoid tip position and glenoid version. An explanatory model of altered PM biomechanics is offered but requires further validation.

Disclaimers:

Funding: No funding was disclosed by the authors.
Conflicts of interest: The authors, their immediate families, and any research foundation with which they are affiliated have not received any financial payments or other benefits from any commercial entity related to the subject of this article.

References

1. Ackland DC, Pak P, Richardson M, Pandy MG. Moment arms of the muscles crossing the anatomical shoulder. J Anat 2008;213:383-90. https://doi.org/10.1111/j.1469-7580.2008.00965.x.
2. Ackland DC, Pandy MG. Lines of action and stabilizing potential of the shoulder musculature. J Anat 2009;215:184-97. https://doi.org/10.1111/j.1469-7580.2009.01090.x.
3. Arciero RA, Cruser DL. Pectoralis major rupture with simultaneous anterior dislocation of the shoulder. J Shoulder Elbow Surg 1997;6:318-20.
4. Asal N, Şahan MH. Radiological variabilities in subcoracoid impingement: coracoid morphology, coracohumeral distance, coracoglenoid angle, and coracohumeral angle. Med Sci Monit 2018;24:8678-84. https://doi.org/10.12659/MSM.911470.
5. Beeler S, Hasler A, Götschi T, Meyer DC, Gerber C. Different acromial roof morphology in concentric and eccentric osteoarthritis of the shoulder: a multiplane reconstruction analysis of 105 shoulder computed tomography scans. J Shoulder Elbow Surg 2018;27:e357-66. https://doi.org/10.1016/j.jse.2018.05.019.
6. Bercik MJ, Kruse K, Yalizis M, Gauci MO, Chaoui J, Walch G. A modification to the Walch classification of the glenoid in primary glenohumeral osteoarthritis using three-dimensional imaging. J Shoulder Elbow Surg 2016;25:1601-6. https://doi.org/10.1016/j.jse.2016.03.010.
7. Bigliani LU, Kelkar R, Flatow EL, Pollock RG, Mow VC. Glenohumeral stability. Biomechanical properties of passive and active stabilizers. Clin Orthop 1996;330:13-30.
8. Bjarnison AO, Sørensen TJ, Kallemose T, Barfod KW. The critical shoulder angle is associated with osteoarthritis in the shoulder but not rotator cuff tears: a retrospective case-control study. J Shoulder Elbow Surg 2017;26:2097-102. https://doi.org/10.1016/j.jse.2017.06.001.
9. Bouaicha S, Ehrmann C, Slankamenac K, Regan WD, Moor BK. Comparison of the critical shoulder angle in radiographs and computed tomography. Skeletal Radiol 2014;43:1053-6. https://doi.org/10.1007/s00256-014-1888-4.
10. Chalmers PN, Salazar D, Steger-May K, Chamberlain AM, Yamaguchi K, Keener JD. Does the critical shoulder angle correlate with rotator cuff tear progression? Clin Orthop Relat Res 2017;475:1608-17. https://doi.org/10.1007/s11999-017-5249-1.
11. Chan K, Knowles NK, Chaoui J, Gauci MO, Ferreira LM, Walch G, et al. Characterization of the Walch B3 glenoid in primary osteoarthritis. J Shoulder Elbow Surg 2017;26:909-14. https://doi.org/10.1016/j.jse.2016.10.003.
12. Cofield RH. Subscapular muscle transposition for repair of chronic rotator cuff tears. Surg Gynecol Obstet 1982;154:667-72.
13. de Jesus JO, Parker L, Frangos AJ, Nazarian LN. Accuracy of MRI, MR arthrography, and ultrasound in the diagnosis of rotator cuff tears: a meta-analysis. AJR Am J Roentgenol 2009;192:1701-7. https://doi.org/10.2214/AJR.08.1241.
14. Domos P, Checchia CS, Walch G. Walch B0 glenoid: pre-osteoarthritis posterior subluxation of the humeral head. J Shoulder Elbow Surg 2018;27:181-8. https://doi.org/10.1016/j.jse.2017.08.014.
15. Donnellan CP, Scott MA, Antoun M, Wallace WA. Physiotherapy and botulinum toxin injections prior to stabilization surgery for recurrent atraumatic anteroinferior shoulder dislocation with abnormal muscle patterning. Shoulder & Elbow 2012;4:287-90. https://doi.org/10.1111/j.1758-5740.2012.00200.x.
16. Friedman RJ, Hawthorne KB, Genez BM. Use of computerized tomography in the measurement of glenoid version. J Bone Joint Surg Am 1992;74:1032-7.
17. Gerber C, Terrier F, Ganz R. The role of the coracoid process in the chronic impingement syndrome. J Bone Joint Surg Br 1985;67:703-8.
18. Gomide LC, Carmo TCD, Bergo GHM, Oliveira GA, Macedo IS. Relationship between the critical shoulder angle and the development of rotator cuff lesions: a retrospective epidemiological study. Rev Bras Ortop 2017;52:423-7. https://doi.org/10.1016/j.rboe.2017.06.002.
19. Heuberer PR, Plachel F, Willinger L, Moroder P, Lakey P, Pauzenberger L, et al. Critical shoulder angle combined with age predict five shoulder pathologies: a retrospective analysis of 1000 cases. BMC Musculoskelet Disord 2017;18:259. https://doi.org/10.1186/s12891-017-1559-4.
20. Hopkins CM, Azar FM, Mulligan RP, Hollins AM, Smith RA, Throckmorton TW. Computed tomography and magnetic resonance imaging are similarly reliable in the assessment of glenohumeral arthritis and glenoid version. Arch Bone Jt Surg 2021;9:64-9. https://doi.org/10.22038/abjs.2020.38922.2035.
21. Hughes RE, Bryant CR, Hall JM, Wening J, Huston LJ, Kuhn JE, et al. Glenoid inclination is associated with full-thickness rotator cuff tears. Clin Orthop Relat Res 2003:86-91. https://doi.org/10.1097/00003086-200302000-00016.
22. Jaggi A, Noorani A, Malone A, Cowan J, Lambert S, Bayley I. Muscle activation patterns in patients with recurrent shoulder instability. Int J Shoulder Surg 2012;6:101-17. https://doi.org/10.4103/0973-6042.106221.
23. Kim JH, Gwak HC, Kim CW, Lee CR, Kwon YU, Seo HW. Difference of critical shoulder angle (CSA) according to minimal rotation: can minimal rotation of the scapula Be allowed in the evaluation of CSA? Clin Orthop Surg 2019;11:309-15. https://doi.org/10.4055/cios.2019.11.3.309.
24. Konrad GG, Jolly JT, Labriola JE, McMahon PJ, Debski RE. Thoracohumeral muscle activity alters glenohumeral joint biomechanics during active abduction. J Orthop Res 2006;24:748-56. https://doi.org/10.1002/jor.20062.
25. Konrad GG, Sudkamp NP, Kreuz PC, Jolly JT, McMahon PJ, Debski RE. Pectoralis major tendon transfers above or underneath the conjoint tendon in

subscapularis-deficient shoulders. An in vitro biomechanical analysis. J Bone Joint Surg Am 2007;89:2477-84. https://doi.org/10.2106/JBJS.F.00811.
26. Kozin SH. Correlation between external rotation of the glenohumeral joint and deformity after brachial plexus birth palsy. J Pediatr Orthop 2004;24:189-93. https://doi.org/10.1097/00004694-200403000-00011.
27. Labriola JE, Lee TQ, Debski RE, McMahon PJ. Stability and instability of the glenohumeral joint: the role of shoulder muscles. J Shoulder Elbow Surg 2005;14:32S-8S. https://doi.org/10.1016/j.jse.2004.09.014.
28. Leite MJ, Pinho AR, Sá MC, Silva MR, Sousa AN, Torres JM. Coracoid morphology and humeral version as risk factors for subscapularis tears. J Shoulder Elbow Surg 2020;29:1804-10. https://doi.org/10.1016/j.jse.2020.01.074.
29. Li X, Xu W, Hu N, Liang X, Huang W, Jiang D, et al. Relationship between acromial morphological variation and subacromial impingement: a three-dimensional analysis. PLoS One 2017;12:e0176193. https://doi.org/10.1371/journal.pone.0176193.
30. Mahylis JM, Entezari V, Jun B-J, Iannotti JP, Ricchetti ET. Imaging of the B2 glenoid: an assessment of glenoid wear. J Shoulder Elbow Arthroplasty 2019;3:2471549219861811. https://doi.org/10.1177/2471549219861811.
31. McMahon PJ, Lee TQ. Muscles may contribute to shoulder dislocation and stability. Clin Orthop Relat Res 2002;(403 Suppl):S18-25. https://doi.org/10.1097/00003086-200210001-00003.
32. Meyer DC, Riedo S, Eckers F, Carpeggiani G, Jentzsch T, Gerber C. Small anteroposterior inclination of the acromion is a predictor for posterior glenohumeral erosion (B2 or C). J Shoulder Elbow Surg 2019;28:22-7. https://doi.org/10.1016/j.jse.2018.05.041.
33. Moor BK, Bouaicha S, Rothenfluh DA, Sukthankar A, Gerber C. Is there an association between the individual anatomy of the scapula and the development of rotator cuff tears or osteoarthritis of the glenohumeral joint?: a radiological study of the critical shoulder angle. Bone Joint J 2013;95-B:935-41. https://doi.org/10.1302/0301-620X.95B7.31028.
34. Moor BK, Wieser K, Slankamenac K, Gerber C, Bouaicha S. Relationship of individual scapular anatomy and degenerative rotator cuff tears. J Shoulder Elbow Surg 2014;23:536-41. https://doi.org/10.1016/j.jse.2013.11.008.
35. Nath RK, Mahmooduddin F, Liu X, Wentz MJ, Humphries AD. Coracoid abnormalities and their relationship with glenohumeral deformities in children with obstetric brachial plexus injury. BMC Musculoskelet Disord 2010;11:237. https://doi.org/10.1186/1471-2474-11-237.
36. Ozel O, Hudek R, Abdrabou MS, Werner B, Gohlke F. The implications of the glenoid angles and rotator cuff status in patients with osteoarthritis undergoing shoulder arthroplasty. BMC Musculoskelet Disord 2020;21:668. https://doi.org/10.1186/s12891-020-03690-8.
37. Page P. Shoulder muscle imbalance and subacromial impingement syndrome in overhead athletes. Int J Sports Phys Ther 2011;6:51-8.
38. Pearl ML, Edgerton BW. Glenoid deformity secondary to brachial plexus birth palsy. J Bone Joint Surg Am 1998;80:659-67. Erratum in: J Bone Joint Surg Am 1998 Oct;80(10):1555-667.
39. Rhee SM, Kim JY, Kim JY, Cho SJ, Kim JH, Rhee YG. The critical shoulder angle: can it be sufficient to reflect the shoulder joint without the humeral head? J Shoulder Elbow Surg 2019;28:731-41. https://doi.org/10.1016/j.jse.2018.08.039.
40. Ricchetti ET, Hendel MD, Collins DN, Iannotti JP. Is premorbid glenoid anatomy altered in patients with glenohumeral osteoarthritis? Clin Orthop Relat Res 2013;471:2932-9. https://doi.org/10.1007/s11999-013-3069-5.
41. Richards DP, Burkhart SS, Campbell SE. Relation between narrowed coracohumeral distance and subscapularis tears. Arthroscopy 2005;21:1223-8. https://doi.org/10.1016/j.arthro.2005.06.015.
42. Sabesan VJ, Callanan M, Youderian A, Iannotti JP. 3D CT assessment of the relationship between humeral head alignment and glenoid retroversion in glenohumeral osteoarthritis. J Bone Joint Surg Am 2014;96:e64. https://doi.org/10.2106/JBJS.L.00856.
43. Sada K, Eto M, Chiba K, Kuwano Y, Kajiyama S, Osaki M. Morphological characteristics of the acromion and the coracoid process in the scapula analyzed by 3D-CT: relationship to rotator cuff tear (Abstract only). J Shoulder Elbow Surg 2018;27:1537. https://doi.org/10.1016/j.jse.2018.05.013.
44. Scalise JJ, Codsi MJ, Bryan J, Iannotti JP. The three-dimensional glenoid vault model can estimate normal glenoid version in osteoarthritis. J Shoulder Elbow Surg 2008;17:487-91. https://doi.org/10.1016/j.jse.2007.09.006.
45. Sinha A, Higginson DW, Vickers A. Use of botulinum A toxin in irreducible shoulder dislocation caused by spasm of pectoralis major. J Shoulder Elbow Surg 1999;8:75-6.
46. Soldado F, Kozin SH. The relationship between the coracoid and glenoid after brachial plexus birth palsy. J Pediatr Orthop 2005;25:666-70. https://doi.org/10.1097/01.bpo.0000164873.41485.19.
47. Stamiris D, Stamiris S, Papavasiliou K, Potoupnis M, Tsiridis E, Sarris I. Critical shoulder angle is intrinsically associated with the development of degenerative shoulder diseases: a systematic review. Orthop Rev (Pavia) 2020;12:8457. https://doi.org/10.4081/or.2020.8457.
48. Tetreault P, Krueger A, Zurakowski D, Gerber C. Glenoid version and rotator cuff tears. J Orthop Res 2004;22:202-7. https://doi.org/10.1016/S0736-0266(03)00116-5.
49. Torrens C, Alentorn-Geli E, Sanchez JF, Isart A, Santana F. Decreased axial coracoid inclination angle is associated with rotator cuff tears. J Orthop Surg (Hong Kong) 2017;25:2309499017690329. https://doi.org/10.1177/2309499017690329.
50. Torstensen ET, Hollinshead RM. Comparison of magnetic resonance imaging and arthroscopy in the evaluation of shoulder pathology. J Shoulder Elbow Surg 1999;8:42-5.
51. van der Sluijs JA, van Ouwerkerk WJ, de Gast A, Wuisman PI, Nollet F, Manoliu RA. Deformities of the shoulder in infants younger than 12 months with an obstetric lesion of the brachial plexus. J Bone Joint Surg Br 2001;83:551-5.
52. Viehöfer AF, Snedeker JG, Baumgartner D, Gerber C. Glenohumeral joint reaction forces increase with critical shoulder angles representative of osteoarthritis-A biomechanical analysis. J Orthop Res 2016;34:1047-52. https://doi.org/10.1002/jor.23122.
53. Viehöfer AF, Gerber C, Favre P, Bachmann E, Snedeker JG. A larger critical shoulder angle requires more rotator cuff activity to preserve joint stability. J Orthop Res 2016;34:961-8. https://doi.org/10.1002/jor.23104.
54. Walch G, Ascani C, Boulahia A, Nové-Josserand L, Edwards TB. Static posterior subluxation of the humeral head: an unrecognized entity responsible for glenohumeral osteoarthritis in the young adult. J Shoulder Elbow Surg 2002;11:309-14. https://doi.org/10.1067/mse.2002.124547.
55. Walch G, Badet R, Boulahia A, Khoury A. Morphologic study of the glenoid in primary glenohumeral osteoarthritis. J Arthroplasty 1999;14:756-60.
56. Walker K, Simcock X, Jun BJ, Iannott J, Ricchetti E. Progression of glenoid morphology in glenohumeral osteoarthritis. J Bone Joint Surg 2018;100:49-56. https://doi.org/10.2106/JBJS.17.00064.
57. Watanabe A, Ono Q, Nishigami T, Hirooka T, Machida H. Association between the critical shoulder angle and rotator cuff tears in Japan. Acta Med Okayama 2018;72:547-51. https://doi.org/10.18926/AMO/56371.
58. Waters PM, Smith GR, Jaramillo D. Glenohumeral deformity secondary to brachial plexus birth palsy. J Bone Joint Surg Am 1998;80:668-77.
59. Watson AC, Jamieson RP, Mattin AC, Page RS. Magnetic resonance imaging based coracoid morphology and its associations with subscapularis tears: a new index. Shoulder Elbow 2019;11:52-8. https://doi.org/10.1177/1758573217744170.
60. Yanagawa T, Goodwin CJ, Shelburne KB, Giphart JE, Torry MR, Pandy MG. Contributions of the individual muscles of the shoulder to glenohumeral joint stability during abduction. J Biomech Eng 2008;130:021024. https://doi.org/10.1115/1.2903422.